UDC 539.4

Accelerating Effects of Cyclic Creep Due to the Alternative Load Compared with Constant Load for CD 304L

A. H. Daei-Sorkhabi[a,1] and F. Vakili-Tahami[b]

[a] Department of Mechanical Engineering, Tabriz Branch, Islamic Azad University, Tabriz, Iran

[b] Department of Mechanical Engineering, University of Tabriz, Tabriz, Iran

[1] amirsorkhabi@gmail.com

УДК 539.4

Сравнительная оценка ускоренных эффектов циклической ползучести в стали CD-304L в условиях переменного и постоянного нагружений

А. Х. Дае-Сорхаби[а], Ф. Вакили-Тахами[б]

[а] Исламский университет Азад, Тебриз, Иран

[б] Тебризский университет, Тебриз, Иран

На основании результатов испытаний на одноосное растяжение выполнена сравнительная оценка ускоренных эффектов циклической ползучести в условиях переменного и постоянного нагружений для аустенитной нержавеющей стали 304L, широко используемой в энергетике и нефтехимической промышленности из-за ее повышенных характеристик сопротивления высокотемпературной ползучести и усталости. Образцы для испытаний получены из холоднотянутых прутков, материал соответствует спецификации ASTM A276-05A. Испытания проводились при температурах 687, 717 и 737°C в условиях знакопеременного и постоянного нагружений. Изучены эффекты переменной нагрузки и времени выдержки нагрузки на механическое поведение материала и характеристики усталости и ползучести. Полученные результаты подтверждают сильное взаимовлияние механизмов ползучести и усталости. Было установлено, что при высоких температурах повреждение материала по механизму ползучести доминирует даже в случае испытаний с очень короткой выдержкой. Кроме того, было показано, что при увеличении времени выдержки увеличивается скорость деформации ползучести и, следовательно, снижается долговечность образцов. Результаты доказывают, что переменные нагрузки существенно увеличивают скорость деформации ползучести и снижают долговечность по сравнению с постоянными нагрузками, обеспечивающими такой же уровень средних напряжений.

Ключевые слова: холоднотянутая сталь 304L, нержавеющая сталь, переменная нагрузка, ползучесть, малоцикловая усталость и ползучесть, выдержка постоянной нагрузки.

Introduction. Many engineering parts, which find applications in power generation and petrochemical plants, operate at high temperature under mechanical loads. In practice, level of operating temperature or the mechanical load may vary with time. Therefore, different mechanisms of failure can occur, which depend on the nature and history of termomechanical loadings. The important failure mechanisms from this point of view are as follows:

(i) fatigue, which is usually faced when the engineering part operates at temperatures below $0.5T_{melt}$ (T_{melt} is melting temperature in Kelvin) and at alternating load with low stresses. Engineering components are often subjected to fatigue loading under stress-

controlled conditions. The existing models describe the fatigue of engineering components including the Goodman equation [1, 2], the modified Goodman equations [1, 3], the Smith–Watson– Topper parameter [4], the Walker parameter [5], and Dowling equation [6];

(ii) creep, which occurs at high temperatures (above $0.5T_{melt}$) under mechanical loads. Creep implies a time-dependant plasticity: after a sufficient elapse of time, either the viscoplastic strain becomes so large that the original shape of the structure is altered, or the creep rupture occurs. Creep is critical in a number of applications, for example, components used in power-generating systems and chemical plants, where the service temperature is high. Different models have been proposed, which explain creep behavior of materials [7];

(iii) elastic shakedown behavior, in which plastic deformation takes place during running in (contact between solid surfaces), while the steady state is perfectly elastic due to residual stresses or strain-hardening. Plastic shakedown behavior is one, in which the steady state is a closed elastic-plastic loop, with no net accumulation of plastic deformation. Except for the initial loading cycles, during which plastic strains may occur, no further deformation increment occurs on the application of loading cycles. Shakedown will occur when the ratcheting fails to occur [8];

(iv) ratcheting behavior is one in which the steady state is an open elastic-plastic loop, with the material accumulating a net strain during each cycle. The accumulation of cyclic deformation is called ratcheting and is defined as a cycle-by-cycle accumulation of plastic strain with the application of cyclic load characterized by constant stress amplitude with a nonzero mean stress. After a sufficient number of cycles, the total strain (displacement) becomes so large that the original shape of the structure is altered, thereby making the structure unserviceable. The development of cyclic plasticity models for prediction of ratcheting strain has received a considerable attention in the past decades, and many models have been suggested. The models by Chaboche and by Ohno and Wang, both based on the Armstrong and Frederick nonlinear kinematic hardening rule, are among the earlier models often cited [9–13].

In practice, most of the engineering components are subjected to the combination of these types of loadings. Therefore, it is important to study the mechanical behavior of materials or even engineering components and the interaction of these mechanisms under the combined thermomechanical loadings. Many engineering components, such as gas turbine blades, operate at high temperature under alternating loads with a low frequency. This type of loading, which is known as “low cycle fatigue-creep,” is the subject of many research studies, especially during the last decade [14–17]. Due to the viscoplastic behavior of the materials at high temperature, shakedown or ratcheting should not be excluded in these studies.

The interaction of damage mechanisms due to the fatigue and creep is an important factor that limits the life of engineering parts. Ignoring the mutual interaction between these mechanisms may lead to erroneous lifetime predictions. Conservative predictions, however, unnecessarily increase the cost of production and maintenance of such systems. Therefore, a realistic assessment of lifetime is critical for the prevention of failures. In some studies, the ASME code method has been used for predicting the creep–fatigue life [14, 15]. This method is not exact, insofar as it’s basis is strictly phenomenological, with no mechanistic component [14]. Many investigators have examined creep-fatigue crack initiation and propagation modes in general. Some of them focused on studying the effect of specific parameters, such as hold time or creep stress effect, environment, orientation, geometry, and material parameters [18–21]. For example, Kaae [21] has carried out low-cycle fatigue tests on alloy 800H in the temperature range of 22–760°C. Alloy 800 is an austenitic Fe–Ni–Cr alloy with higher Ni and Cr contents than conventional stainless steels. It is widely used for many high-temperature applications in such areas, as petrochemical processing, electrical power generation, and solar energy systems. In their tests, the axial strain was cycled between equal positive and negative values.

Sabour and Bhat [18] have investigated the creep-fatigue interaction for aircraft components. They have proposed innovative mathematical models to predict the operating life of these components, specifically gas turbine blades that are subjected to creep-fatigue at high temperatures.

Since most of engineering components, which work at high temperature, operate under alternating load, it is important to know their behavior at this condition. On the other hand, most of the available data for creep are at constant load or stress. Therefore, it expedient to estimate the creep life-time and deformation of the parts at alternating load based on the experimental data obtained at constant stress. This particular issue is the major aim of the present paper. For this purpose, by using a series of uniaxial creep tests under alternating load, the behavior of cold-drawn 304L stainless steel (CD 304L SS) at high temperature has been determined experimentally. Uniaxial creep tests have been carried out at 687, 717, and 737°C under constant and alternating loads. The effects of alternating load and the hold time on the mechanical behavior of the material have been studied to investigate the mutual effect of two damage mechanisms.

1. **Creep-Fatigue Damage**. The most common method to calculate creep-fatigue damage is based on the linear superposition of these damages, which leads to the linear life-fraction rule, which forms the basis of the ASME Boiler and Pressure Vessel Code, Section III, Code Case N-47 [22]. This approach combines the damage summations of Robinson for creep and of Miner for fatigue as follows [18]:

$$\sum \frac{N}{N_f} + \sum \frac{t}{t_r} = D, \tag{1}$$

where N/N_f is the cyclic portion of the life fraction, in which N is the number of cycles at a given strain (or stress) range and N_f is the pure fatigue life at that strain (or stress) range. The time-dependent creep-life fraction is t/t_r, where t is the time at a given stress and temperature, and t_r is the time to rupture at that stress and temperature, and D is the cumulative damage index. Failure is presumed to occur when $D = 1$. If Eq. (1) is valid, then a straight line of the type shown in Fig. 1 between the fatigue and creep life fractions should be expected [18]. The linear behavior shown in Fig. 1 is the ideal type, which can be depicted by Eq. (1). However, the true behavior of most materials is non-linear which can be approximated using a bi-linear model as shown in Fig. 1. Most materials manifest a drastic lifetime reduction under the combined effect of creep and fatigue damages. For example, as it can be seen in Fig. 1, when the $N/N_f = 0.4$, the t/t_f value calculated via Eq. (1) is expected to be 0.6. However, due to accumulation of creep damage with loading cycles, a more realistic lifetime is predicted by the bi-linear model as $t/t_r = 0.35$. On the other hand, when the number of cycles is too low ($N/N_f < 0.2$), the fatigue damage is negligible, and therefore the lifetime becomes closer to the ideal value obtained from the linear equation.

The life-fraction rule given by Eq. (1) has no mechanistic basis and is therefore, material-dependent. It also assumes that tensile and compressive hold periods are equally damaging, whereas most of the experimental results show minor damage levels in compression. Other effects, such as the strain softening or hardening behavior, the effect of prior plasticity on subsequent creep, and the order of loading, have not been accounted for by this rule, which therefore, in general, provides only approximate results. In spite of these limitations, this rule of damage summation is very popular because it is easy to use and requires only a standard fatigue *S–N* diagram and creep stress-rupture curves. To overcome the above shortcomings, it is necessary to carry out creep tests under alternating load, in which the specimen is exposed to a high temperature for a long period. This type of tests has been carried out in this research, in order to obtain results that are more realistic.

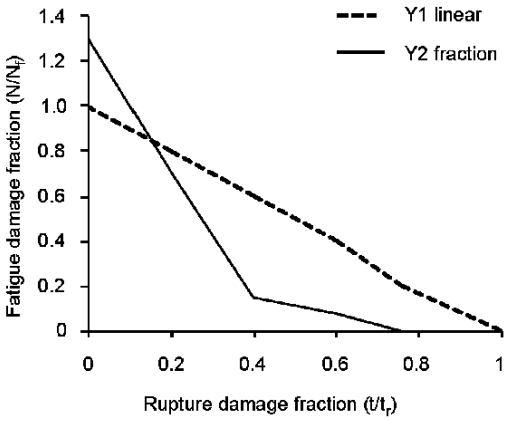

Fig. 1. Creep rupture/low cycle fatigue damage interaction curve for 1Cr–Mo–V rotor steel at 450℃ [18].

2. **Material and Experimental**. Type 304 stainless steel is the most widely used alloy of the austenitic stainless steel group. It is a variation of the basic 18-8 grade, type 302, with a higher chromium and lower carbon content. Lower carbon minimizes the chromium carbide precipitation due to the welding and its susceptibility to intergranular corrosion. Type 304L is an extra low-carbon variation of type 304 with a 0.03% maximum carbon content that eliminates carbide precipitation due to the welding. As a result, this alloy can be used in the "as-welded" condition, even in severe corrosive environment. 304L has slightly lower mechanical properties than type 304. The maximum temperature to which 304 and 304L can be exposed continuously without appreciable scaling is about 899℃. For intermittent exposure, the maximum exposure temperature is about 816℃. The hardness of type 304L does not increase considerably by heat treatment; and it can be annealed by heating to 1038–1121℃ followed byrapid cooling. Cold worked parts can be stress relieved at 399℃ for 1/2 to 2 h [23].

In the current research, creep test specimens have been obtained directly from new austenitic 304L stainless steel cold drawn bars, which have been solution, annealed at 1050℃. The material conforms to ASTM A276-05A specifications. Chemical composition of this material is given in Table 1.

T a b l e 1

Chemical Composition of 304L Stainless Steel in Weight Percent

Composition	C	Si	Mn	P	S	Cr	Mo	Ni	Cu	N	V
Standard	0.019	0.41	1.75	0.036	0.006	18.28	0.34	8.04	–	0.04	–
Tested (CD 304L SS)	0.025	0.42	1.80	0.035	0.015	17.80	0.27	8.10	0.76	–	0.19

Here both the standard values [23] and those, which have been obtained from quant-metric measurements for the specimens under investigation, are given. The test specimens have been machined out from the bars according to the ASTM E8M-04 [24] with gauge length of 100 mm and diameter of 10 mm (see Fig. 2).

2.1. ***Test Machine***. Uniaxial creep tests have been carried out using 5000 kg, AMSLER creep test machine according to the ASTM E139 [25] standard. Its lever-arm loading ratio is 25:1 with load accuracy of ± 0.5%. The temperature range of the furnace or chamber of the machine is up to 1000℃ with the accuracy of ±0.5℃. The testing machine also provides displacement–time graphs with the accuracy of ±1.0 μm. The maximum

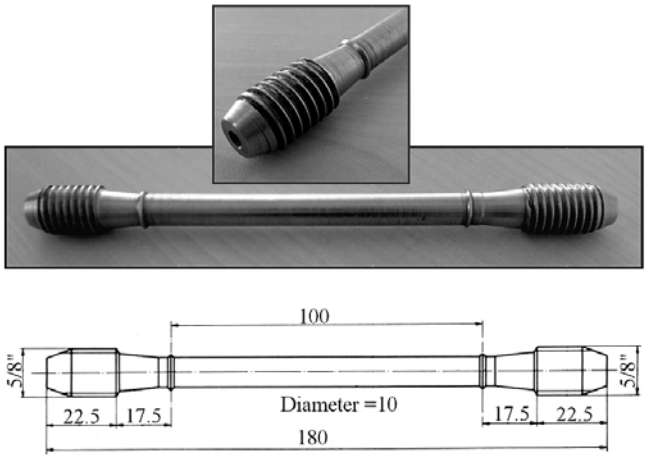

Fig. 2. Uniaxial creep test specimen according to the ASTM E8M-04 [24] with gauge length of 100 mm and diameter of 10 mm. (Dimensions are in mm.)

extension of the specimen is 10 mm (see Fig. 3). To apply alternating load, the capability of this machine is improved by using a moving weight (1000 kg) along the lever-arm (Fig. 4). The speed and location of this weight, as well as the frequency of the alternating load, can be pre-programmed using a computer-controlled electronic system. Using this system and additional alternating axial load of 0 to 10,000 N can be applied to the specimen.

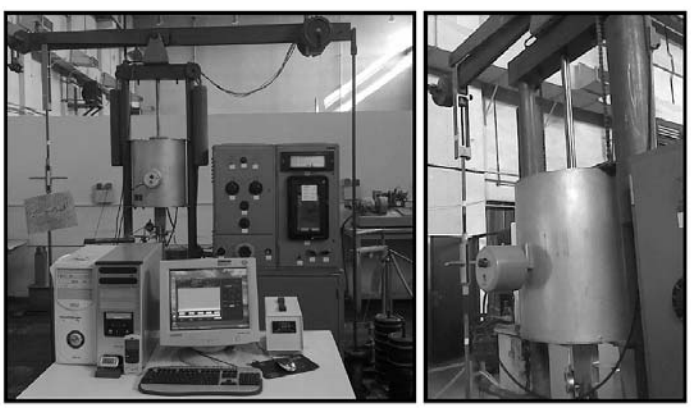

Fig. 3. Uniaxial creep test machine: 5000 kg, AMSLER according to the ASTM E139 standard [25].

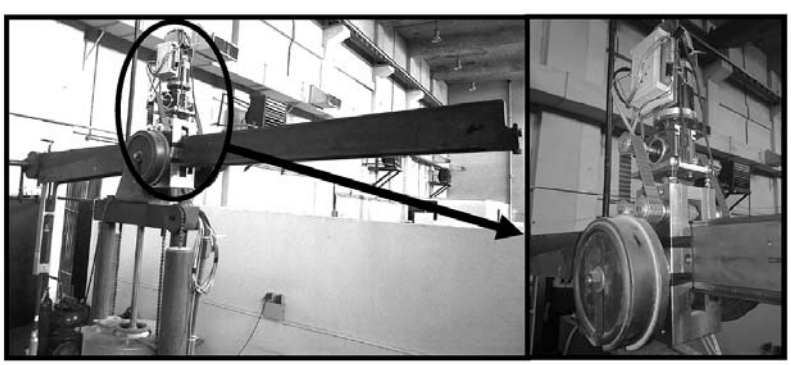

Fig. 4. Alternating moving load along the lever-arm of uniaxial creep test machine.

2.2. ***Test Conditions***. In order to investigate the creep and creep-fatigue behavior of the material, three groups of tests are carried out:

(i) constant load creep, where the uniaxial load and temperature are constant during the tests;

(ii) creep-fatigue, where the temperature level is constant but the uniaxial load is alternating with very short hold time;

(iii) alternating load creep, where the temperature level is constant, but the uniaxial load is alternating with relatively long hold times.

Although the operating temperature for engineering components manufactured from 304L is usually below 650°C in industry, but to reduce the testing times to an achievable limit, the tests have been carried out at higher temperature levels of 687, 717, and 737°C, in view that the creep mechanism is the same, since these temperatures are below the recrystallization level [26]. Also, to avoid the initial plastic deformation, in all tests, the maximum stress is below the yield stress of the material at the same temperature.

3. **Results**.

3.1. ***High Temperature Mechanical Tests***. To study the high temperature mechanical behavior of cold drawn 304L, a series of tensile tests at high temperatures have been carried out and the results are given in Table 2.

T a b l e 2

Mechanical Properties of CD 304L SS

Test No.	T, °C	S_u,* MPa	S_y,* MPa	S_e, MPa
1	25	675	425	310*
2	517	430	346	198**
3	617	370	299	170**
4	687	300	252	138**
5	717	268	228	123**
6	817	158	117	72**

* obtained experimentally; ** obtained using Eq. (2).

Standard high-cycle fatigue tests at room temperature have been carried out to obtain the endurance limit of the material. Since the endurance limit of steels are proportionally related to the ultimate tensile strength [27], by knowing the latter at high temperatures, the former can be estimated. Hence, the endurance limit at high temperatures $(S_e)_T$ have been estimated using Eq. (2) based on the endurance limit at room temperature $(S_e)_{T=25°C}$ and ultimate strength of the material S_u at high and room temperatures, which have been obtained experimentally,

$$(S_e)_T = \left(\frac{(S_u)_T}{(S_u)_{T=25°C}}\right)(S_e)_{T=25°C}. \qquad (2)$$

3.2. ***Constant Load Creep Tests***. Table 3 presents the experimental data for constant load creep tests. In this table, the stress $\sigma = F_0/A_0$ is obtained using the constant load (F_0) and initial cross section of the specimen (A_0). In all tests, the stress is below the yield stress of the material at the same temperature. Creep failure in engineering components can be regarded in two ways: when the time to rupture, t_r, has been reached or the time, $t_{creep\ strain=C\%}$, at which the creep strain reaches a critical level of $C\%$. In most of the engineering components, the latter condition plays a major role; and therefore, it has been used in this study. Since the maximum extension of the specimen is 10 mm (total strain of 10%) in the creep-testing-machine, all the tests have been carried out until the true creep

strain of 3% has been reached or $t = t_{creep\ strain=3\%}$. At this amount of deformation, most of engineering components would be regarded as failed. The summary of the creep test results is given in Table 3.

Also, the minimum creep strain rate, $\dot{\varepsilon}_{ss}$, for each test has been given in this table. Figures 5 and 6 show the variation of the creep strain with time at 717 and 687°C, respectively. The results given in Table 3 and Figs. 5 and 6 show that by increasing the stress or temperature, time to reach the 3% creep strain decreases significantly.

T a b l e 3

Constant Load Creep Test Results for CD 304L SS at High Temperatures

Test No.	T, °C	σ,* MPa	$t_{creep\ strain=1\%}$,* h	$t_{creep\ strain=3\%}$,* h	$\dot{\varepsilon}_{ss}$, %/h
7	737	86.5	27	65	$3.65 \cdot 10^{-2}$
8	717	142.0	1.5	4.25	$9.36 \cdot 10^{-1}$
9	717	112.0	11	25	$9.41 \cdot 10^{-2}$
10	717	86.5	185	327	$3.81 \cdot 10^{-3}$
11	717	56.5	3671	NA**	$2.65 \cdot 10^{-4}$
12	687	142.0	68	132	$1.31 \cdot 10^{-2}$
13	687	86.5	1390	NA**	$5.61 \cdot 10^{-4}$

* obtained experimentally; ** not available (the test has been stopped before reaching 3% strain).

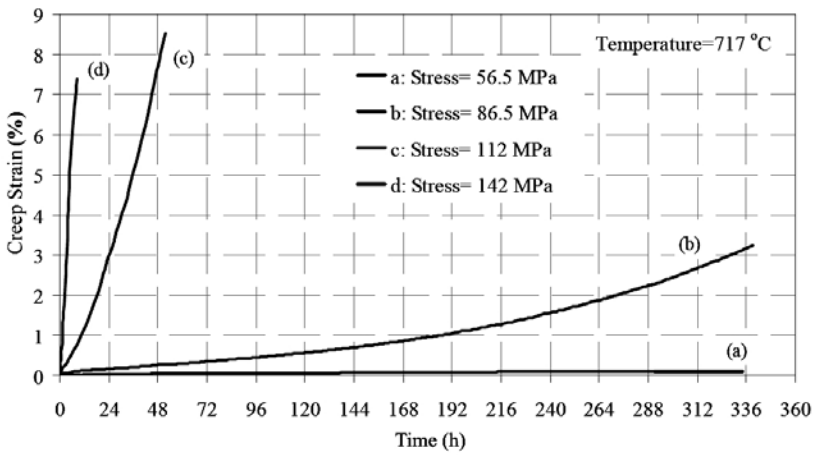

Fig. 5. Creep strain variation of CD 304L SS for constant load creep tests at 717°C.

3.3. ***Creep Tests at Alternating Loads***. Table 4 presents the experimental data for creep tests at alternating loads. In this table, the following parameters have been used to define the test conditions:

$$\begin{aligned} \sigma_{\max} &= F_{\max}/A_0, \\ \sigma_{\min} &= F_{\min}/A_0, \\ \sigma_m &= (\sigma_{\max} + \sigma_{\min})/2, \\ \sigma_a &= (\sigma_{\max} - \sigma_{\min})/2, \end{aligned} \tag{3}$$

T a b l e 4

Alternating Load Creep Test Results for CD 304L SS at High Temperatures

Test No.	T, °C	$\sigma_{\max}$,* MPa	$\sigma_{\min}$,* MPa	t_h, s	Creep strain = 1%		Creep strain = 3%		$\dot{\varepsilon}_{ss}$, m/(m/s)
					Total time (h)	N_i, cycles	Total time (h)	N_i, cycles	
14	717	142	31	2	45	1306	115	3338	$2.19 \cdot 10^{-2}$
15	717	112	1	2	292	8477	513	14893	$2.07 \cdot 10^{-3}$
16	717	112	1	1800	33.1	32	80.6	78	$3.12 \cdot 10^{-2}$
17	717	112	1	2700	29	19	73.5	54	$3.34 \cdot 10^{-2}$
18	717	112	1	3600	25	12	55	27	$4.49 \cdot 10^{-2}$
19	687	142	31	2	1332	38670	NA**	NA**	$1.34 \cdot 10^{-4}$

* obtained experimentally; ** not available (the test has been stopped before reaching 3% strain).

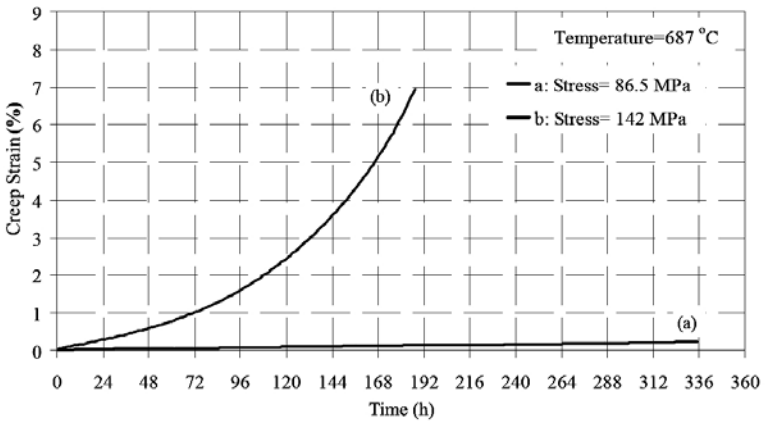

Fig. 6. Creep strain variation of CD 304L SS for constant load creep tests at 687℃.

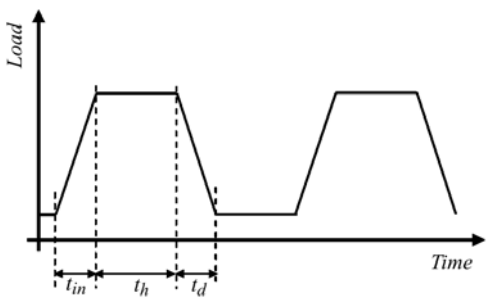

Fig. 7. Schematic diagram of load–time variation used to apply alternating loads.

where $F_{\max}$ and $F_{\min}$ refer to the maximum and minimum applied loads also, σ_m and σ_a refer to average and alternating stress. Since, most of the engineering components operate at tensile stress, and knowing the fact that the creep damage is mostly due to this type of loading, in all tests the minimum stress is above 1 MPa to avoid any compressive load. In addition, all tests are load controlled as shown schematically in Fig. 7. In this figure, definition of parameters such as load-increasing time, t_{in}, load-decreasing time, t_d, and holding time, t_h, are presented. In all tests $t_i = t_d = 60$ s.

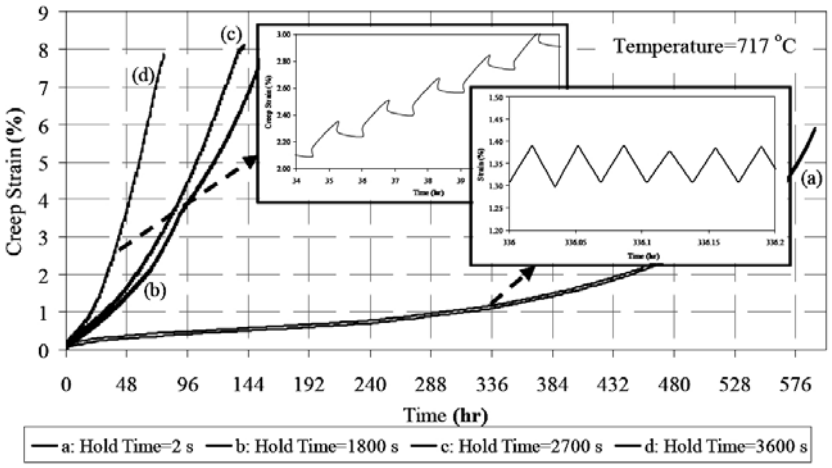

Fig. 8. Variation of the creep strain with time for alternating load tests under different hold times.

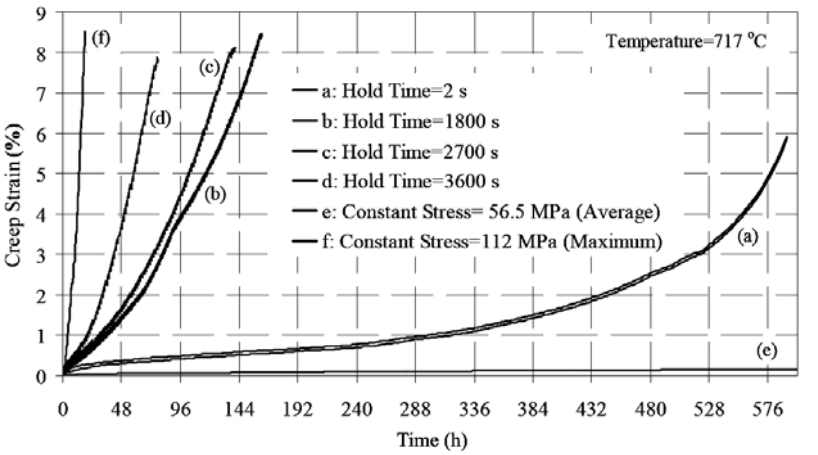

Fig. 9. Variation of the creep strain with time for constant (average and maximum) and alternating load.

Figure 8 shows the variation of the creep strain with time for alternating load tests at 717°C. The stresses for alternating load-tests change between 1 to 112 MPa. This figure shows that by increasing hold time, creep strain rate increases significantly. To compare different behaviors of the material, the results for constant load creep tests with 112 MPa (maximum stress) and 56.5 MPa (average stress) are also included in Fig. 9.

The summary of the test results is given in Table 4. As it can be seen, in all tests, the specimens reach the creep lifetime limit (creep strain of 1 or 3%) without facing fatigue fracture. For example, in test No. 14, in spite of the fact that the hold time is very short (two seconds), even after 3338 cycles, fatigue fracture has not occurred and during this period, which lapsed 115 h, the creep strain has reached 3% limit. The same trend has been observed in test No. 15, and after 14,893 cycles, the creep lifetime criterion being satisfied without facing fatigue fracture.

4. **Discussion**. To evaluate the level of creep-fatigue damage of the tests, the ASME Code Case N-47 has been used. This code is based on the use of interaction diagrams such as that shown in Fig. 1 for the material under consideration. The estimation of the total damage is also obtained by the use of Eq. (1).

As it can be seen in Table 4, tests Nos. 14, 15, and 19 have very short hold times (two seconds) and therefore they can be considered as fatigue tests at high temperature. Based on the Manson–Coffin equation [16], the pure fatigue damage is related to the number of cycles and the range of strain change in each cycle or $N_f = B(\Delta\varepsilon)^m$, where B and m are material constants. Hence, by increasing $\Delta\varepsilon$, the fatigue damage will increase. It can be seen in Fig. 10 (also in Table 5) that the strain range $\Delta\varepsilon$ at each cycle for tests with $t_h = 2$ s remains almost constant (for example from 0.06 to 0.07% for 687°C, maximum stress of 142 MPa, minimum stress of 31 MPa) but their average values are increased by increasing temperature (for example compare the strain rang for test No. 14 and 19) or mean stress σ_m (compare test No 14 and 15). Therefore, it can be concluded that both increasing temperature and mean stress level will lead to a shorter fatigue-life. Fatigue-life for each test can be calculated using either Manson–Coffin equation, or fatigue life diagrams for 304L material [18]. The estimated fatigue-lives given in Table 5 have been obtained using diagrams provided in ASME Code Case N-47 and for these tests, they are equal or above 10^6 cycles. Therefore, the fatigue damage value, $\sum N_i / N_f$, is very low. Also in Table 6, the amount of creep damage, $\sum t_i / t_{creep\ strain=1\%}$, are given, in which the creep lifetime is considered to be the life to reach 1% creep strain. It can be seen that due to the high temperature and stress level for these tests, the creep damage is much higher than the fatigue one, despite very short hold times. Clearly, by increasing hold time, the role of creep damage will increase and this failure mechanism will be the dominant one.

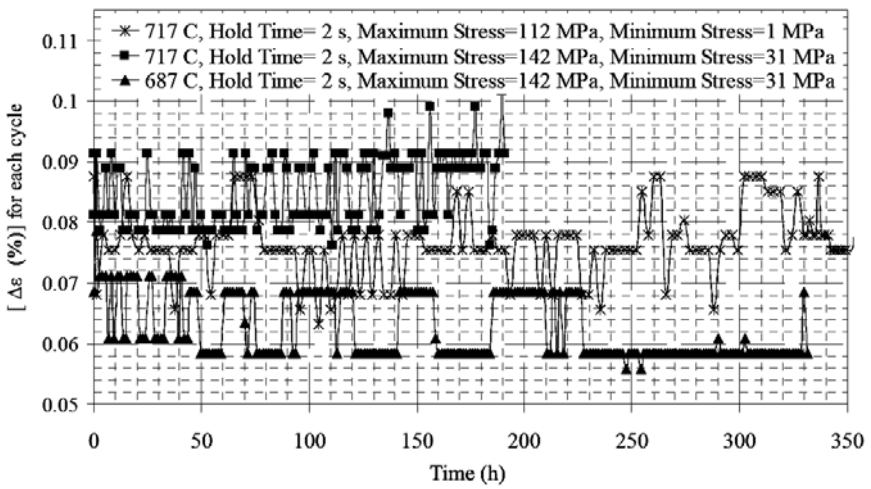

Fig. 10. Variation of strains for each cycle with time for three alternating load tests.

Moreover, comparison of the results for tests Nos. 15–18 shows the effect of holding time on the material creep behavior. Although the stress and temperature levels for these tests are the same, but due to the increasing hold time, creep strain rate has increased significantly and therefore the creep lifetime is reduced. For example, for test No. 15 with $t_h = 2$ s, $t_{creep\ strain=3\%}$ is 513 h, but for test No. 18 with $t_h = 3600$ s, $t_{creep\ strain=3\%}$ reduces to 55 h.

The test results can be compared using the power law form of constitutive equation to estimate the steady state creep strain rate:

$$\dot{\varepsilon}_{ss} = C\sigma^n, \tag{4}$$

Table 5

Fatigue Damage Evaluation in Tests with a Short Hold Time of 2 s

Test No.	T, °C	σ_{max}, MPa	σ_{min}, MPa	t_h, s	N_i, cycles	$\Delta\varepsilon$, mm/mm	Fatigue life N_f, cycles	Fatigue damage $\sum N_i/N_f$
14	717	142	31	2	1306	$8.64 \cdot 10^{-4}$	10^6	$1.306 \cdot 10^{-3}$
15	717	112	1	2	8477	$7.54 \cdot 10^{-4}$	above 10^6	$8.477 \cdot 10^{-3}$
19	687	142	31	2	38670	$6.35 \cdot 10^{-4}$	above 10^6	$3.867 \cdot 10^{-2}$

Table 6

Creep Damage Evaluation in Tests with a Short Hold Time of 2 s

Test No.	T, °C	σ_{max}, MPa	σ_{min}, MPa	t_h, s	Creep strain = 1%			Creep damage $\sum t_i/t_{creep\ strain=1\%}$
					N_i, cycles	$t_i = t_h N_i$, h	t_f at max stress, h	
14	717	142	31	2	1306	0.73	1.5	0.49
15	717	112	1	2	8477	4.71	11.0	0.43
19	687	142	31	2	38670	21.48	68.0	0.32

where $\dot{\varepsilon}_{ss}$ is the creep strain rate (in h^{-1}), σ is stress (in MPa), C and n are material constants. Comparison of the results for test No. 11 in Table 3 and test No. 15 in Table 4 highlights the significant effect of alternating load on the creep strain rate and lifetime of the material.

Comparative analysis of the results for tests Nos. 10 and 11 in Table 3 and tests Nos. 14 and 15 in Table 4 also demonstrates the effect of average stress level on the creep lifetime of the material under alternating load. For example, by increasing the applied constant stress from 56.5 to 86.5 MPa, creep strain rate increases by a factor of 14.377 and time for 1% creep strain reduces by factor of 0.05. This trend can also be seen in comparing the results for tests with alternative stress.

The effect of holding time on creep strain rate can be observed by comparing the results for tests No. 15 to No. 18. For example by increasing hold time from 2 to 3600 s, steady state creep strain rate increases by a factor of 21.69 with decrease in time to reach 1% creep strain rate by a factor 0.09.

Conclusions. A set of constant and alternating load creep tests have been carried out to predict creep behavior of cold-drawn 304L SS. The test results show the difference in creep behavior of the material under constant and alternating loads.

1. It has been shown that at high temperature and at stress levels below the yield point at the associated temperature, the specimens have reached creep lifetime limit (creep strain of 1 or 3%) without facing fatigue fracture. For example, in test No. 14, in spite of the fact that the hold time is very short (two seconds), even after 3338 cycles, fatigue fracture has not occurred and during this period which lapsed 115 h, the creep strain has reached 3% limit.

2. The results highlight the major impact of the alternating loads in increasing creep strain rate and reducing the creep lifetime when compared with the constant load tests at the same average stress. For example, in test No. 11, at 717°C and constant stress of 56.5 MPa,

creep life for 1% strain is 3673 h, whereas for test No. 15 with alternating load (56.5 MPa mean stress and 55.5 MPa alternating stress, two second hold time) creep life for 1% strain is 292 h or 12.6 times shorter. Hence, estimating creep lifetime for alternating loads based on the average stress will lead to erroneous result.

3. It has been shown that by increasing the hold time, the creep strain rate increases and consequently, the creep lifetime is reduced.

4. The results show that due to the high temperature and stress level for these tests, the creep damage is much higher than the fatigue damage despite very short hold times.

Р е з ю м е

На основі результатів випробувань на одноосьовий розтяг виконано порівняльну оцінку прискорених ефектів циклічної повзучості в умовах змінного і постійного нагружений для аустенітної нержавіючої сталі 304L, широко використовуваної в енергетиці та нафтохімічної промисловості через її підвищених характеристик опору високотемпературної повзучості і втоми. Зразки для випробувань отримано з холоднотягнутих прутків, матеріал відповідає специфікації ASTM A276-05A. Випробування проводилися при температурах 687, 717 і 737°C в умовах змінного й постійного навантажень. Вивчено ефекти змінного навантаження та часу витримки на механічну поведінку матеріалу і характеристики втоми й повзучості. Отримані результати підтверджують сильний взаємовплив механізмів повзучості і втоми. Було встановлено, що при високих температурах пошкодження матеріалу за механізмом повзучості домінує навіть у випробуваннях з дуже короткою витримкою. Крім того, було показано, що при збільшенні часу витримки збільшується швидкість деформації повзучості і, отже, знижується довговічність зразків. Результати доводять, що змінні навантаження істотно збільшують швидкість деформації повзучості і знижують довговічність у порівнянні з постійними навантаженнями, що забезпечують такий самий рівень середніх напружень.

1. C. B. Lim, K. S. Kim, and J. B. Seong, "Ratcheting and fatigue behavior of a copper alloy under uniaxial cyclic loading with mean stress," *Int. J. Fatigue*, **31**, No. 3, 501–507 (2009).
2. M. S. Beden, S. Abdullah, A. K. Ariffin, et al., "Fatigue life assessment of different steel-based shell materials under variable amplitude loading," *Eur. J. Sci. Res.*, **29**, No. 1, 157–169 (2009).
3. J. Morrow, "Fatigue properties of metals," in: *Fatigue Design Handbook*, Section 3.2, Publ. No. AE-4, Soc. of Automotive Engineers, Warrendale, PA (1968).
4. R. N. Smith, P. Watson, and T. H. Topper, "A stress-strain function for the fatigue of metal," *J. Mater.*, **5**, No. 4, 767–778 (1970).
5. K. Walker, "The effect of stress ratio during crack propagation for 2024-T3 and 7075-T6 aluminum," in: *Effects of Environment and Complex Load History on Fatigue Life*, ASTM STP 462, Philadelphia (1970), pp. 1–14.
6. N. E. Dowling, "Mean stress effects in stress-life and strain-life fatigue," in: Proc. of the Third Int. Sea Fatigue Congress, Sao Paulo, Brazil (2004).
7. J. T. Boyle and J. Spence, *Stress Analysis for Creep*, Butterworth & Co. Ltd. (1983).
8. K. S. Basaruddin and L. C. Wooi, "Uniaxial ratcheting of mild steel under cyclic tension," in: Proc. of Int. Conf. on Applications and Design in Mechanical Engineering (ICADME), Batu Ferringhi, Penang, Malaysia (2009).
9. J. L. Chaboche, "On some modifications of kinematic hardening to improve the description of ratcheting effects," *Int. J. Plast.*, **7**, 661–678 (1991).

10. N. Ohno and J. D. Wang, "Kinematic hardening rules with critical state of dynamic recovery. Part I: Formulations and basic features for ratcheting behavior," *Int. J. Plast.*, **9**, 375–390 (1993).
11. X. Chen, R. Jiao, and K. S. Kim, "On the Ohno–Wang kinematic hardening rules for multiaxial ratcheting modeling of medium carbon steel," *Int. J. Plast.*, **21**, 161–184 (2004).
12. P. J. Armstrong and C. A. Frederick, *A Mathematical Representation of the Multiaxial Bausinger Effect*, CEGB Report No. RD/B/N 731 (1966).
13. X. Chen, D.-H. Yu, and K. S. Kim, "Experimental study on ratcheting behavior of eutectic tin–lead solder under multiaxial loading," *Mater. Sci. Eng. A*, **406**, 86–94 (2005).
14. D. W. Kim, J. H. Chang, and W. S. Ryu, "Evaluation of the creep-fatigue damage mechanism of type 316L and type 316LN stainless steel," *Int. J. Press. Vess. Piping*, **85**, 378–384 (2008).
15. D. W. Kim, H. Y. Lee, Ch. G. Park, and J. H. Lee, "Creep-fatigue test of a SA316SS structure and comparative damage evaluations based upon elastic and inelastic approaches," *Int. J. Press. Vess. Piping*, **85**, 550–556 (2008).
16. S. Holdsworth, "Creep-fatigue interaction in power plant steels," *Mater. High Temp.*, **28**, No. 3, 197–204 (2011).
17. S. R. Holdsworth, R. P. Skelton, and B. A. Dogan, "Code of practice for the measurement and analysis of high strain creep-fatigue short crack growth," *Mater. High Temp*., **27**, No. 4, 265–283 (2010).
18. M. H. Sabour and R. B. Bhat, "Lifetime prediction in creep-fatigue environment," *Mater. Sci. Poland*, **26**, No. 3, 563–584 (2008).
19. R. Valentin, D. Barker, and M. Osterman, "Model for life prediction of fatigue-creep interaction," *Microelectr. Reliab.*, **48**, 1831–1836 (2008).
20. J. Ewald, S. Sheng, A. Klenk, and G. Schellenberg, "Engineering guide to assessment of creep crack initiation on components by two-criteria-diagram," *Int. J. Press. Vess. Piping*, **78**, 937–949 (2001).
21. J. L. Kaae, "High-temperature low-cycle fatigue of alloy 800H," *Int. J. Fatigue*, **31**, 332–340 (2009).
22. *ASME Boiler and Pressure Vessel Code, Section III, Division 1 – Subsection NH, Class 1 Components in Elevated Temperature Service*, ASME, New York (2001).
23. *ASTM A276-05a. Standard Specification for Stainless Steel Bars and Shapes*, Vol. 02.04, ASTM International, West Conshohocken, PA (2005).
24. *ASTM E8M-04. Standard Test Methods for Tension Testing of Metallic Materials (Metric)*, ASTM International, West Conshohocken, PA (2004).
25. *ASTM E139-06. Standard Test Methods for Conducting Creep, Creep-Rupture, and Stress-Rupture Tests of Metallic Materials*, ASTM International, West Conshohocken, PA (2006).
26. A. Le Pécheur, F. Curtit, M. Clavel, et al., "Thermo-mechanical FE model with memory effect for 304L austenitic stainless steel presenting microstructure gradient," *Int. J. Fatigue*, 45, 106–115 (2012).
27. Y. L. Lee, M. E. Barkey, and H. T. Kang, *Metal Fatigue Analysis Handbook: Practical Problem – Solving Techniques for Computer-Aided Engineering*, Chapter 4: *Stress-Based Uniaxial Fatigue Analysis*, Butterworth–Heinemann (2011).

Received 09. 04. 2014